Catalysis Letters
https://doi.org/10.1007/s10562-020-03177-0

Highly Efficient Conversion of Renewable Levulinic Acid to *n*-Butyl Levulinate Catalyzed by Sulfonated Magnetic Titanium Dioxide Nanotubes

Fei-Feng Mao[1] · Wenguang Zhao[2] · Duan-Jian Tao[1] · Xianxiang Liu[2]

Received: 28 January 2020 / Accepted: 10 March 2020

Abstract
A new solid acid catalyst Fe_3O_4@TNTs-SO_3H was successfully prepared, characterized, and applied for efficient conversion of renewable levulinic acid to *n*-butyl levulinate, serving as a promising liquid fuel additive. This catalyst was demonstrated to show high catalytic activity and afford *n*-butyl levulinate with a yield of 94.6% under optimum conditions.

Graphic Abstract

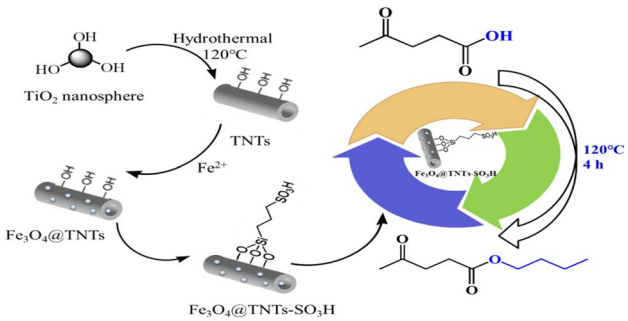

Keywords Titanate nanotubes · *n*-Butyl levulinate · Esterification · Magnetic catalyst · Solid acid

1 Introduction

With the growing consumption of fossil resources, great efforts have been devoted to the conversion of abundant and renewable biomass resources into high value-added chemicals [1]. As one of the most important chemicals derived from biomass resources, alkyl levulinates are well known to have widespread applications in many fields such as plasticizing agents, solvents, odorous substances, and fuel additives [2, 3]. In addition, alkyl levulinates contain two functional groups (a ketone group and an ester group), which are prominent building blocks for the synthesis of various chemicals and drugs [3, 4]. Alkyl levulinates were mainly obtained by direct esterification of levulinic acid with alcohols in the presence of acid catalysts, and enzymatic methods were also documented recently [5]. Homogeneous acids such as sulfuric acid, hydrochloric acid, phosphoric acid and

Fei-Feng Mao and Wenguang Zhao have contributed equally to this work.

✉ Duan-Jian Tao
djtao@jxnu.edu.cn

✉ Xianxiang Liu
lxx@hunnu.edu.cn

[1] College of Chemistry and Chemical Engineering, Jiangxi Normal University, Nanchang 330022, China

[2] National & Local Joint Engineering Laboratory for New Petro-Chemical Materials and Fine Utilization of Resources, Key Laboratory of the Assembly and Application of Organic Functional Molecules of Hunan Province, College of Chemistry and Chemical Engineering, Hunan Normal University, Changsha 410081, China

Published online: 16 March 2020

p-toluenesulfonic acid were reported for the esterification of levulinic acid [6], but these homogeneous catalytic systems demonstrated some disadvantages such as the severe corrosion and the generation of the waste, which limited their applications [7]. To overcome the above mentioned drawbacks of homogeneous catalytic systems, several types of heterogeneous solid acids catalysts, such as sulfated oxides (SnO_2, ZrO_2, Nb_2O_5, TiO_2) [2], zeolites [8], Zr-containing MOFs [9], porous organic polymeric solid acids [10, 11], sulfonated carbon nanotubes [12] and Wells–Dawson heteropolyacid [13], were developed for the esterification of levulinic acid. Although these heterogeneous catalysts could be separated from the reaction mixture in comparison with homogeneous acid catalysts, there reported methods still suffered some disadvantages. For example, some heterogeneous catalysts were not active for the esterification of levulinic acid due to the inherit weak acidity. In addition, some heterogeneous acid catalysts were difficult to recycle, which required the use of the tedious filtration or centrifugation process. Therefore, the development of novel heterogeneous catalysts for the esterification of levulinic acid is still highly desirable particularly magnetic acid catalysts.

Titanium dioxide (TiO_2) is chemically stable, which have been used as the acid catalysts for chemical reactions [14]. Among different types of TiO_2, titanium dioxide nanotubes (TNTs) endows larger specific surface area and more regular pore structure, which has received a great interest in recent years [15]. Furthermore, in terms of green chemistry, magnetically recoverable catalysts have emerged as a potent and persuasive option due to their merits such as excellent catalytic performance, stability and magnetic recyclability [16–18]. In this work, new sulfonic acid functionalized magnetic titanium dioxide nanotubes (Fe_3O_4@TNTs-SO_3H, see Scheme 1) were successfully prepared and studied for the esterification of levulinic acid. The catalyst amount, reaction temperature, and reactant molar ratio were found to have significant effects on this catalytic system. Under the optimal conditions, 94.6% of *n*-butyl levulinate could be obtained. Our results suggest that Fe_3O_4@TNTs-SO_3H could be used as a good candidate for alkyl levulinate production from biomass-derived platform molecules.

2 Experimental Section

All reagents were of analytical grade and used as received: levulinic acid (Aladdin, 99%), 3-trimethoxysilylpropanethiol (APTMS, Aladdin, 99%), TiO_2 nanoparticles (Anatase, > 99.9%), $FeCl_2{\cdot}4H_2O$ (Tianjin fengchuan chemical reagent technology Co., Ltd, 99%), $NH_3{\cdot}H_2O$, acetone, *n*-butyl alcohol, NaOH, HCl, H_2O_2, toluene, methanol (Sinopharm Chemical Reagent Co. Ltd, 99%).

2.1 Preparation and Characterization of Catalysts

Preparation of TNT: TiO_2 nanotubes (TNTs) were prepared by hydrothermal method [19]. 1.5 g of TiO_2 was mixed with 60 mL of 10 mol/L NaOH aqueous solution, followed by hydrothermal treatment at 150 °C in a Teflon-lined autoclave for 24 h. The treated powders were washed thoroughly with 0.1 mol/L HCl aqueous solution until the pH value of the washing solution lower than 7. The attained suspension was then centrifuged. The solid sample was washed with distilled water until the pH of the rinsing solution close to neutral, and then subsequently filtered and dried at 60 °C.

Preparation of Fe_3O_4@TNTs: 0.5 g of the prepared TNTs was initially dispersed into 15 mL of aqueous solution of $FeCl_2{\cdot}4H_2O$ (0.128 mol/L). Then, $NH_3{\cdot}H_2O$ (2.5%, 10 mL) was slowly added with a stirring and kept at 85 °C for 30 min. The sample was thoroughly washed with deionized water for

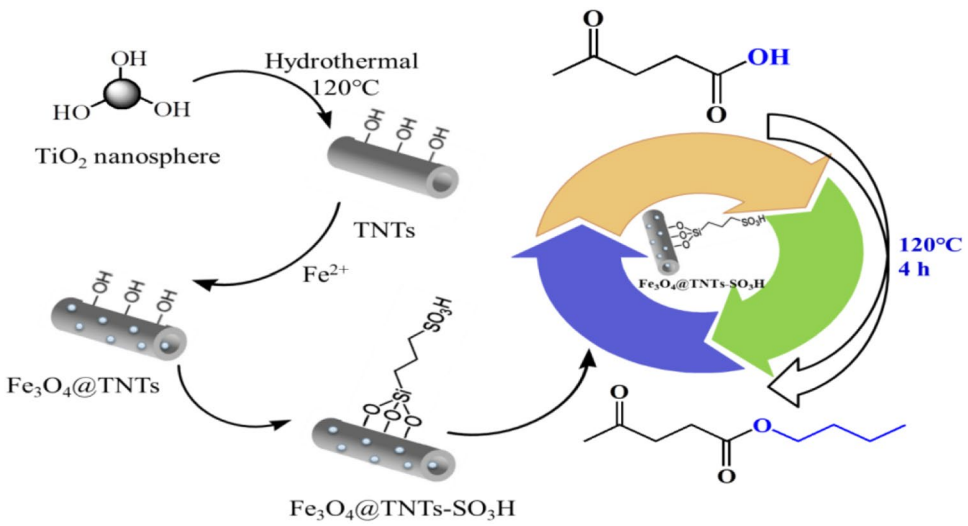

Scheme 1 Synthesis of magnetic titanium dioxide nanotubes and used for the esterification reaction of levulinic acid with *n*-butyl alcohol

several times, and separated by an external magnet and finally dried at 100 °C.

Preparation of Fe_3O_4@TNTs-SO_3H: The obtained Fe_3O_4@TNTs (1.5 g) were dispersed into 20 mL of toluene. Then 4 mL of 3-trimethoxysilylpropanethiol was added to the mixture. The mixture was refluxed for 24 h with a stirring. After that, the solid product was collected by a magnet, washed with acetone and dried at 100 °C. Finally, the as-synthesized product was dispersed into 20 mL of methanol at room temperature, followed by the addition of 4 mL of H_2O_2 (4 mL), and then refluxed for 24 h. Finally, the as-formed Fe_3O_4@TNTs-SO_3H acid catalyst was achieved after being washed with deionized water and acetone and dried at 100 °C.

Fourier transform infrared spectra (FT-IR) were collected on a Nicolet 370 infrared spectrophotometer and the samples were prepared by the KBr pellet method. Powder X-ray diffraction (XRD) patterns was collected on a Bruker X-ray diffraction (XRD) spectroscopy using Cu Kα radiation (λ = 1.5418 Å). Thermogravimetric and differential thermogravimetric (TG-DTG) curves were recorded on a Netzsch Model STA 409PC instrument. The transmission electron microscopy (TEM) images were obtained using FEI Tecnai G2 F20. The magnetic of Fe_3O_4@TNTs-SO_3H catalyst was investigated using vibrating sample magnetometry (VSM, LakeShore7404).

2.2 Catalytic Reactions

Catalytic experiments were performed in 10 mL round bottom flask, which was coupled with a reflux condenser using the following general procedure. Typically, the Fe_3O_4@TNTs-SO_3H catalyst was added into the mixture of levulinic acid (LA, 10 mmol) and *n*-butanol (50 mmol). Then the reaction was started at the desired reaction temperature for a certain time. After reaction, the reaction mixture was cooled down to room temperature, and the products were analyzed quantitatively by Shimadzu GC-2014 gas chromatograph (GC). The gas chromatograph was equipped with a HP-5 capillary column (30 m length, 0.32 mm internal diameter, 0.50 μm film thickness) and a fame ionization detector (FID). The temperatures of the injection port, the oven and the detector were set to 250 °C, 180 °C, and 250 °C, respectively. The mixture in the reaction solution were detected by GC–MS, a Shimadzu GC system equipped with a capillary (30 m length, 0.32 mm internal diameter, 0.25 μm film thickness).

LA conversion and *n*-butyl levulinate (BL) yield are defined as follows:

$$\text{LA conversion} = (1 - \text{moles of LA/moles of starting LA}) \times 100\%$$

$$n-\text{butyl levulinate yield} = \text{Moles of } n-\text{butyl levulinate/moles of starting LA} \times 100\%$$

3 Results and Discussion

3.1 Characterization of Catalysts

TNTs, Fe_3O_4@TNTs and Fe_3O_4@TNTs-SO_3H were first characterized by FT-IR analysis (Fig. 1). It can be seen that all the samples have a wide peak around 3407 cm^{-1}, which was due to the –OH stretching vibration of the water physically adsorbed on the surfaces or located in the sandwich group. The peak at 1625 cm^{-1} was assigned to the O–H deformation vibration of H–O–H and Ti–OH bonds [20]. In addition, the peak around 482 cm^{-1} could be interpreted as the crystal lattice vibration of TiO_6 octahedra [21, 22]. Compared the FT-IR spectra of TNTs and Fe_3O_4@TNTs, two new peaks were observed in Fe_3O_4@TNTs-SO_3H, and the sharp peaks around 1141 cm^{-1} and 1041 cm^{-1} can be ascribed to O=S=O bond symmetry and anti-symmetric stretching vibration in the –SO_3H group [23, 24] This suggests that the sulfonic acid group has successfully bonded to the magnetic titanium nanotubes.

The purity and the phase of the various stepwise-prepared materials from TNTs to Fe_3O_4@TNTs-SO_3H were compared via thermogravimetric analysis ranging from room temperature to 700 °C (Fig. 2). The TG-DTG results of TNTs and Fe_3O_4@TNTs exhibit an initial weight loss at about 110 °C, corresponding to the loss of the physically adsorbed water. Additionally, an exothermic peak of DTG curve pattern at about 210 °C is attributed to some traces of the densification of amorphous TiO_2 network by the shrinkage of interlayer distance, confirming the nanotube formation [25]. For comparison, Fe_3O_4@TNTs-SO_3H shows two additional weight losses at 240–305 °C and 305–600 °C. Meanwhile, a strong

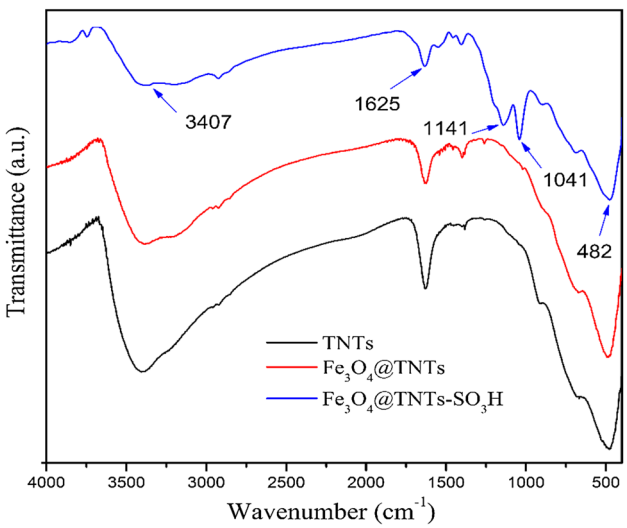

Fig. 1 FT-IR spectra of TNTs, Fe_3O_4@TNTs and Fe_3O_4@TNTs-SO_3H

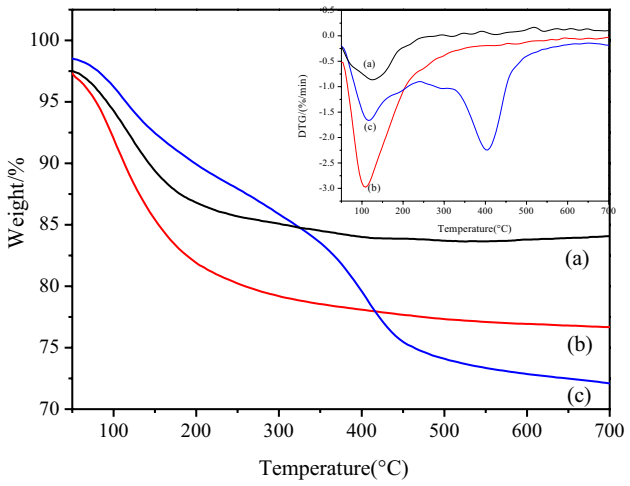

Fig. 2 TG-DTG curves of TNTs (a), Fe_3O_4@TNTs (b), and Fe_3O_4@TNTs-SO_3H (c)

and sharp endothermic DTG signal was observed at 405 °C, corresponding to decomposition of alkyl chain along with SO_3H group, which is consistent with the reported literature [26]. From the TG-DTG results, it is found that Fe_3O_4@TNTs-SO_3H shows an excellent thermal stability, under our reaction conditions as described in the below.

The XRD patterns of the three samples were presented in Fig. 3. All the samples exhibited four peaks at $2\theta = 25.4°$, 37.7°, 38.8° and 48.4°, corresponding to the characteristic diffraction signals of the titanate anotubes [27, 28] with diffraction lines of the cubic spinel phase (101), (004), (112), and (200), respectively (JCPDS card no. 21–1272). For Fe_3O_4@TNTs, peaks at $2\theta = 30.1°$, 35.5°, 57.1° and 62.7° can be attributed to the XRD pattern of the Fe_3O_4 nanoparticles with diffraction lines of the cubic spinel phase (220), (311), (400), (331), (422), and (511), respectively (JCPDS card no. 85–1436) [16]. There was no difference in the XRD patterns of the Fe_3O_4@TNTs and Fe_3O_4@TNTs –SO_3H catalysts.

The TEM and SEM images of TNTs-SO_3H and Fe_3O_4@TNTs-SO_3H were shown in Fig. 4. Figure 4c shows that the nanotubes with outside diameter and inner diameter of approximately 13.3 nm and 5.3 nm, respectively. The magnetic Fe_3O_4 nanoparticles were deposited on the surface and pores of titanium nanotube. These results indicate that the functionalization process has been performed successfully. Furthermore, the amount of acidity of the Fe_3O_4@TNTs-SO_3H catalyst was determined by ion-exchanged method. Firstly, the Fe_3O_4@TNTs-SO_3H was stirred in the saturated NaCl solution to release the H^+ to the solution via the ion-exchange by Na^+. The filtrate was then titrated with a standard NaOH solution. The concentration of HSO_3^- for Fe_3O_4@TNTs-SO_3H was determined to be 1.59 mmol/g.

The magnetic strength of the Fe_3O_4@TNTs-SO_3H catalyst was also investigated using vibrating sample magnetometry (VSM) at room temperature. As shown in Fig. 5, the S-shaped magnetization hysteresis loops indicated the superparamagnetic nature of the prepared catalyst Fe_3O_4@TNTs-SO_3H with immeasurable remanence and coercivity. The saturation magnetization (Ms) value was measured to be 5.6 emu/g. The above data indicated that the Fe_3O_4@TNTs-SO_3H catalyst demonstrated an excellent magnetic property.

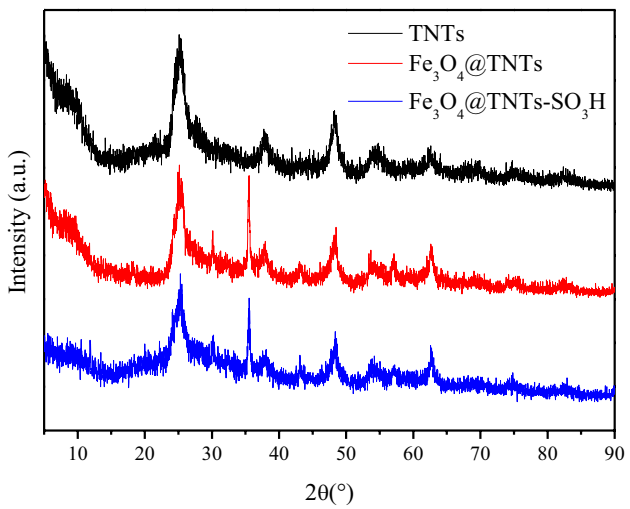

Fig. 3 XRD patterns of TNTs, Fe_3O_4@TNTs and Fe_3O_4@TNTs -SO_3H

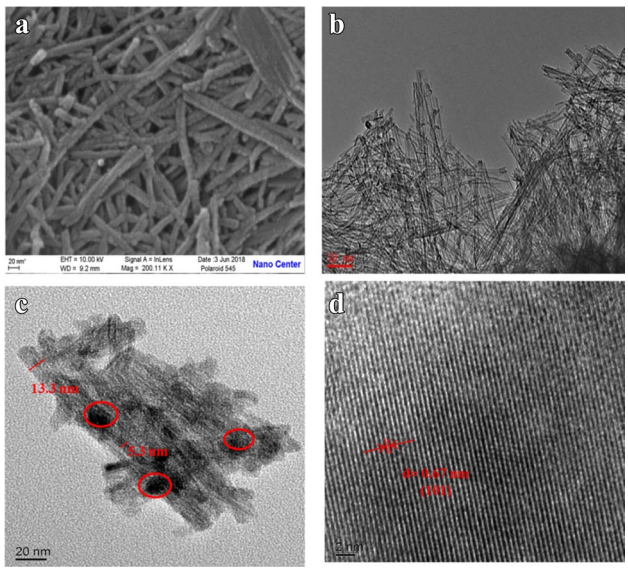

Fig. 4 SEM images of the TNTs-SO_3H (**a**) and TEM images of TNTs-SO_3H (**b**), and Fe_3O_4@TNTs-SO_3H (**c**, **d**)

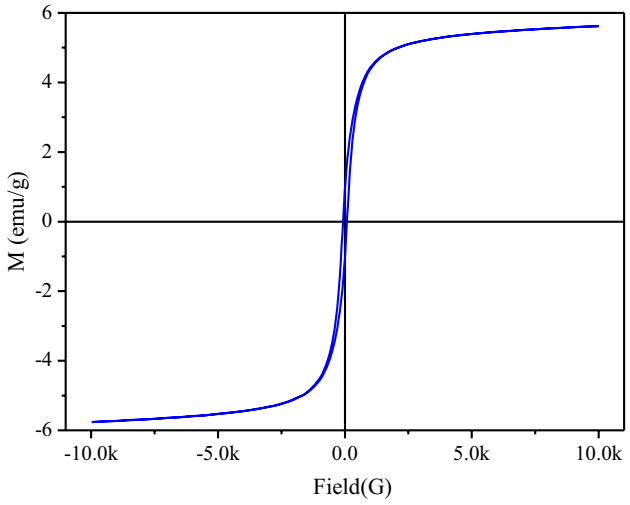

Fig. 5 VSM magnetization curve of Fe_3O_4@TNTs-SO_3H

3.2 Effect of Catalysts on LA Esterification

Figure 6 demonstrated the esterification of levulinic acid (LA) with *n*-butyl alcohol to form *n*-butyl levulinate (BL) at 120 °C by different catalysts. The blank experiment was tested and the LA conversation and the BL yield were calculated to be 46.1% and 40.0%, respectively. These results suggested that the carboxylic acid from LA itself could promote the esterification of with *n*-butyl alcohol. In contrast, the presence of TNTs resulted in higher LA conversion (69.9%) and BL yield (62.1%) in comparison with the blank reaction, which demonstrated that the TNTs had the acidic groups to promote the the esterification reaction of levulinic acid (LA) with *n*-butyl alcohol. Interestingly, it was noted that the Fe_3O_4@TNTs demonstrated slight lower activity for this transformation, probably due to the block of the acidic sites of TNTs by the Fe_3O_4 nanoparticles. With the aim to improve the catalytic activity and facilitate the recycle of heterogeneous catalyst, the magnetic Fe_3O_4@TNTs-SO_3H catalyst with a strong acidity was prepared, and used for the esterification reaction of levulinic acid (LA) with *n*-butyl alcohol. As expected, the Fe_3O_4@TNTs-SO_3H catalyst produced the highest LA conversion was 89.7% with 78.8% BL yield. This implies that the combination of Bronsted acid sites from –SO_3H and Lewis acid sites from TiO_2 and Fe_3O_4 shows moderate acid strength and enough acidic sites and thereby leads to a good yield of BL. In addition, the Fe_3O_4@TNTs-SO_3H catalyst also exhibited the esterification of LA with three primary alcohols such as methanol, ethanol, and propanol with high yields more than 60%.

3.3 Effect of Reaction Time on LA Esterification

We further investigated the time-dependent catalytic performances of Fe_3O_4@TNTs-SO_3H for the esterification of LA with *n*-butanol at 120 °C. As shown in Fig. 7, both the conversion of LA and the yield of BL greatly increased at the early reaction stage, which was due to the high concentration of the substrates at the early reaction stage. For example, the conversion of LA in 23.3% and the yield of BL in 34.4% were obtained within 15 min, while the values significantly increased to 60.1% and 79.1% within 1 h. After 4 h, the conversion of LA and the yield of BL reached 91.9% and 95.5% after 4 h. There is no remarkable change of BL yield and LA conversion after 4 h. Therefore, all of subsequent experiments were performed at 120 °C for 4 h.

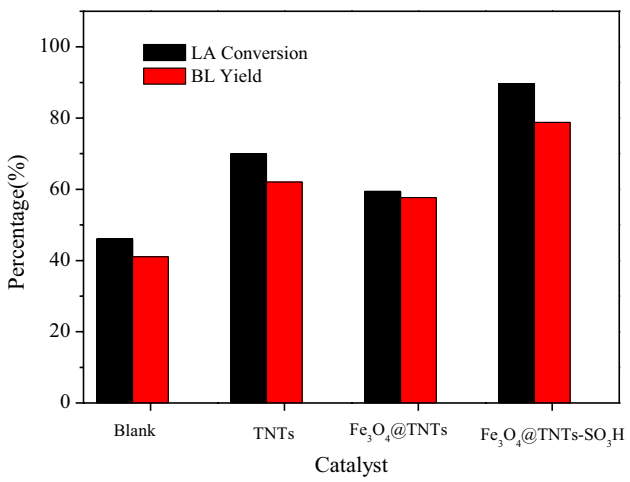

Fig. 6 Effect of catalysts on LA esterification. Reaction conditions: 10 mmol LA, 50 mmol *n*-butanol, 5 wt% catalyst dosage, reflux reaction at 120 °C for 4 h

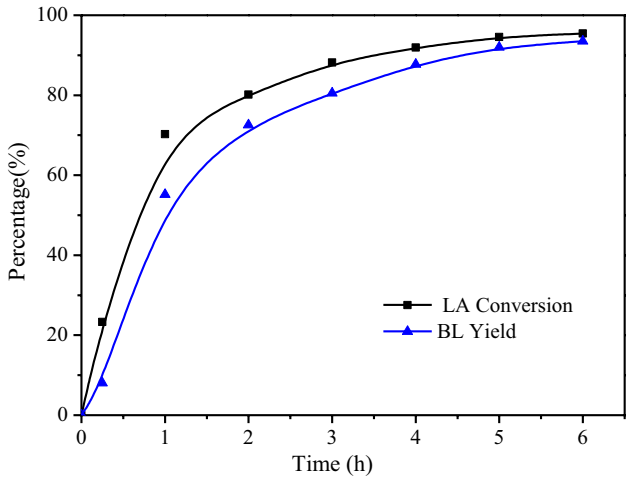

Fig. 7 Effect of reaction time on LA esterification. Reaction conditions: 10 mmol LA, 50 mmol *n*-butanol, 5 wt% catalyst dosage, 120 °C

3.4 Effect of Reaction Temperature on LA Esterification

The influence of reaction temperature on the esterification of LA with *n*-butanol was further investigated and the results are shown in Fig. 8. At a lower temperature of 90 °C, the yield of BL was 33.6% after 4 h with 5 wt% catalyst dosage. The esterification of LA with *n*-butanol was greatly accelerated by the increase of the reaction temperature from 90 to 120 °C, and then a slight increase was observed from 120 to 130 °C. The yield of BL was 80.5% within 4 h at 120 °C, and that was 83.6% at 130 °C. The obtained results indicated that high reaction temperature promoted the LA esterification as well as the BL yield. However, too high a temperature resulted in a higher production cost. Therefore, the temperature was fixed at 120 °C in the following experiments.

3.5 Effect of Catalyst Amount on LA Esterification

The catalytic performance of Fe_3O_4@TNTs-SO_3H catalysts with different catalyst dosage was tested at 120 °C for 4 h, as shown in Fig. 9. It can be found that when the amount of Fe_3O_4@TNTs-SO_3H increased from 1 to 12 wt%, the yield of BL was significantly improved to 86.4%, which could be attributed to the increased active site number. From the perspective of cost, the dosage of the Fe_3O_4@TNTs-SO_3H catalyst used in later experiment is 12 wt%.

3.6 Effect of Reactant Molar Ratio on LA Esterification

Esterification reaction was usually tested under an excess of alcohol so as to achieve higher yields. Herein, the effect of reactant molar ratio on the synthesis of *n*-butyl levulinate was studied over the Fe_3O_4@TNTs-SO_3H catalyst. It was observed from Fig. 10 that the yield of BL increases from 75.4 to 94.6% with the increasing molar ratio of LA to *n*-butanol from 1:1 to 1:5, while it tends to be saturated when increasing *n*-butanol dosage up to 6 eq. This trend was much more obvious at a lower molar ratio of LA to *n*-butanol from 1:1 to 1:2.

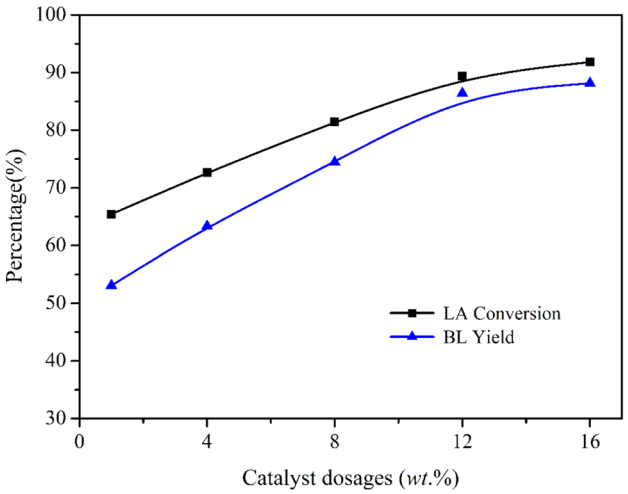

Fig. 9 Effect of catalysts amount on LA esterification. Reaction conditions: 10 mmol LA, 50 mmol *n*-butanol, reflux reaction at 120 °C for 4 h

3.7 Stability Test

The reusability of solid acid catalyst was one of the key factors for evaluating its catalytic performance. Therefore,

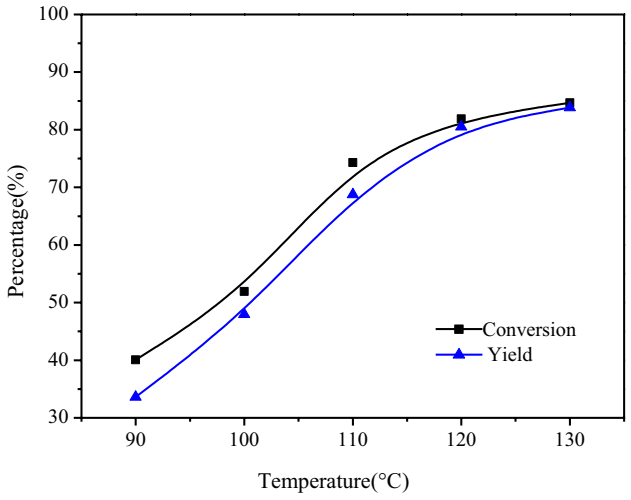

Fig. 8 Effect of reaction temperature on LA esterification. Reaction conditions: 10 mmol LA, 50 mmol *n*-butanol, 5 wt% catalyst dosage, reflux reaction for 4 h

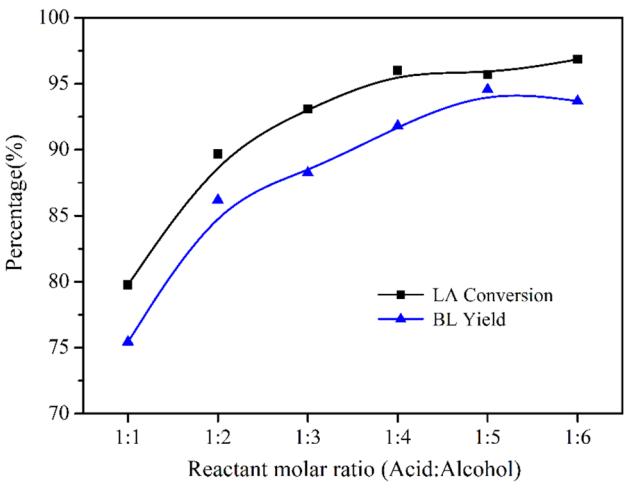

Fig. 10 Effect of reactant molar ratio on LA esterification. Reaction conditions: 10 mmol LA, 50 mmol *n*-butanol, 12 wt% catalyst dosage, reflux reaction at 120 °C for 4 h

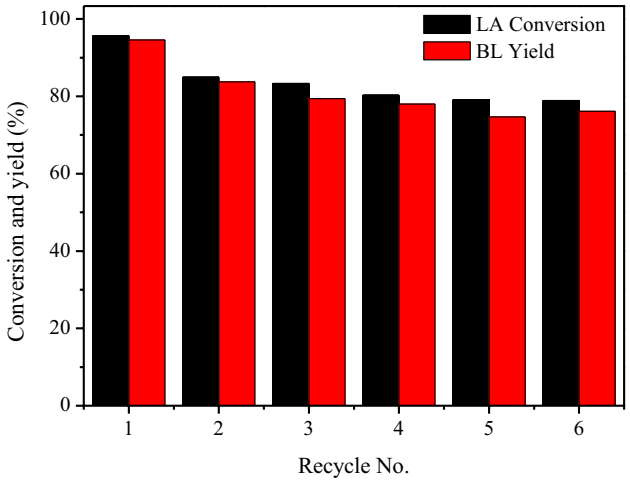

Fig. 11 The results of catalyst recycling experiments. Reaction conditions: 10 mmol LA, 50 mmol *n*-butanol, 12 wt% catalyst dosage, reflux reaction at 120 °C for 4 h

the recycle experiment was carried out under the optimum reaction conditions. The catalyst was recovered and washed by methanol several times. After dried at 60 °C, the recovered catalyst was reused for the next cycle. From the results shown in Fig. 11, it was obvious that the recycled catalyst could be reused for at least six times without considerable decrease of its initial catalytic performance in terms of the LA conversion and BL yield. The result of elemental analysis also confirmed that there was trace of leaching sulfur element in the reaction mixture after hot filtration. The slight decrease in the conversion of LA and yield of BL should be due to the slight loss of Fe_3O_4@TNTs-SO_3H catalyst because of the transferring of catalyst during the regeneration.

4 Conclusions

In this study, we have demonstrated sulfonic acid functionalized magnetic titanium dioxide nanotubes (Fe_3O_4@TNTs-SO_3H) as a novel, green, reusable heterogeneous solid acid catalyst. The structural verification of the catalyst was fully characterized, and the corresponding results suggest that the sulfonic acid functional groups were successfully attached to Fe_3O_4@TNTs. Furthermore, the catalyst showed excellent catalytic performance for esterification of levulinic acid with *n*-butyl alcohol, and the yield of *n*-butyl levulinate could be reached to 94.6%. Meanwhile, the catalyst could be easily separated and reused for six times. We believe that the prepared Fe_3O_4@TNTs-SO_3H has great potential of application in the conversion of biomass derived platform chemicals into valuable bulk chemicals as heterogeneous solid acid catalyst.

Acknowledgements The authors gratefully acknowledge the financial support of the National Natural Science Foundation of China (21606082), Hunan Provincial Natural Science Foundation of China (2018JJ3334), China Postdoctoral Science Foundation (2019M662787), and Research Learning and Innovative Experiment Project of Undergraduates in Hunan Province (201810542040).

Compliance with Ethical Standards

Conflict of interest The authors declare no competing financial interest.

References

1. Liu XX, Xu Q, Liu JY, Yin DL, Su SP, Ding H (2016) Fuel 164:46
2. Fernandes DR, Rocha AS, Mai EF, Mota CJA, Silva VTD (2012) Appl Catal A 425:199
3. Zhang J, Wu SB, Li B, Zhang HD (2012) ChemCatChem 4:1230
4. Demma CP, Ciriminna R, Shiju NR, Rothenberg G, Pagliaro M (2014) Chemsuschem 7:835
5. Kuwahara Y, Fujitani T, Yamashita H (2014) Catal Today 237:18
6. Bart HJ, Reidetschlager J, Schatka K, Lehmann A (1994) Ind Eng Chem Res 33:21
7. Zhou SL, Liu XX, Lai JH, Zheng M, Liu WZ, Xu Q, Yin DL (2019) Chem Eng J 361:571
8. Liu F, Willhammar T, Wang L, Zhu L, Sun Q, Meng X, Wilder CC, Zou X, Xiao FS (2012) J Am Chem Soc 134:4557
9. Cirujano FG, Corma A, Xamena FXL (2015) Chem Eng Sci 124:52
10. Liu F, Huang K, Zheng A, Xiao FS, Dai S (2018) ACS Catal 8:372
11. Liu F, Kong W, Qi C, Zhu L, Xiao FS (2012) ACS Catal 2:565
12. Oliveira BL, Silva VTD (2014) Catal Today 234:257
13. Pasquale G, Vázquez P, Romanelli G, Baronetti G (2012) Catal Commun 18:115
14. Atghia SV, Beigbaghlou SS (2013) J Nano Struct Chem 3:38
15. Kitano M, Nakajima K, Kondo JN, Hayashi S, Hara M (2010) J Am Chem Soc 132:6622
16. Zolfigol MA, Yarie M (2016) Appl Organomet Chem 31:e3598
17. Cheng T, Zhang D, Li H, Liu G (2014) Green Chem 16:3401
18. Karimi B, Mansouri F, Mirzaei HM (2015) ChemCatChem 7:17369
19. Kasuga T, Hiramatsu M, Hoson A, Sekino T, Niihara K (1999) Adv Mater 11:1307
20. Linghu WS, Sun YX, Hai Y, Chang KK, Sheng GD, Hayat T, Alharbi NS, Ma JY (2017) J Mol Liq 244:146
21. Silva TA, Diniz J, Paixão L, Vieira B, Barrocas B, Nunes CD, Monteiro OC (2017) Solid State Sci 63:30
22. He C, Sasaki T, Shimizu Y, Koshizaki N (2008) Appl Surf Sci 254:2196
23. Zhou WL, Yoshino M, Kita H, Okamoto K (2001) Ind Eng Chem Res 40:4801
24. Kolvari E, Koukabi N, Hosseini MM (2015) J Mol Catal A 397:68
25. Muniyappan S, Solaiyammal T, Sudhakar K, Karthigeyan A, Murugakoothan P (2017) Mod Electron Mater 3:174
26. Ng EP, Subari SNM, Marie O, Mukti RR, Juan JC (2013) Appl Catal A 450:34
27. Zhou SL, Jiang DB, Liu XX, Chen YP, Yin DL (2018) RSC Adv 8:3657
28. Lu SX, Zhong H, Mo DM, Hu Z, Zhou HL, Yao Y (2017) Green Chem 19:1371